Efficient 2D stress analysis of an isotropic bolted joint connection with finite dimensions using the Airy stress function

MINH NGUYEN-HOANG, WILFRIED BECKER
Institute of Structural Mechanics
Technical University Darmstadt
Franziska-Braun-Straße 7, 64287 Darmstadt
GERMANY
nguyen-hoang@fsm.tu-darmstadt.de becker@fsm.tu-darmstadt.de

Abstract: Bolted joints are a common mean to connect safety critical parts in the aeronautical industry and therefore require precise stress analysis, which can take place analytically enabling cost-efficient computation. Connections with an even number of plates and a symmetrical setup with respect to the midplane can be modelled as a plate under in-plane loading. The complexity further reduces to a pure plane problem if there is no bending extension coupling. The flux of forces is directed from the bolt towards the clamp, which are both located at finite boundaries. Therefore modelling must be performed within a finite domain. If the material is isotropic this plane boundary value problem can be solved by means of the Airy stress function, which is the focus of the present paper. The geometry is chosen in such a way that additional stress concentrations faded away. At first a solution for the infinite dimensions bolted joint is derived, which is then mirrored in order to cancel stresses in load direction at the straight edges of the finite joint. Thus the load is physically transferred and characteristic field quantities are accurately modelled providing an efficient tool for 2D stress analysis and subsequent net tension failure assessment.

Key–Words: Pin-loaded hole, Airy stress function, Finite dimensions

1 Introduction

Bolted joints are widely used in the aeronautical industry for reasons like inexpensive manufacturing and the ability to disassemble. Nevertheless drilling a hole also introduces a stress raiser, which has to be assessed in stress and subsequent failure analysis.

If the connection contains an even number of plates and has a fully symmetrical setup with respect to the midplane then the bolted joint connection can be modelled as a plate under in-plane loading. This pin-loaded hole problem with pin-plate contact idealised as sinusoidal stress distribution has been treated by many researchers with different levels of complexity such as finite dimensions or material anisotropy. If the material is anisotropic the stress field can be determined by means of Lekhnitskii complex potentials [5], which was solved for both infinite and finite geometry without bending extension coupling [2, 8] reducing the complexity to a plane problem. Contrary in [3] anisotropic problems involving bending extension coupling were solved. If the material is isotropic the stress field can be solved by means of the Airy stress function, which is performed in [1] for infinite dimensions. This solution satisfies the hole boundary conditions and gives a good approximation of its circumferential stresses. Since the stresses in load direction within the net section area rapidly converge to an unphysical value in compression they are not be suitable to asses crack initiation. In [4] the stress field for both infinite dimensions and finite width is developed. The radial stress boundary conditions at the hole are fulfilled whereas those in the shear stresses are unfortunately slightly violated. As taking into account finite width while neglecting effects of finite height a semi-infinite problem is treated whose load transfer should not be used for real problems with finite dimensions.

In the present paper the stress field for a pin-loaded hole in an isotropic plate with finite dimensions is analytically derived using the Airy stress function aiming to satisfy the boundary conditions both at the hole and the straight edges. This is required to physically model the flux of forces and the net section stress decay vital for failure assessment. First, a solution for a joint with infinite dimensions is developed. Afterwards the finite dimensions solution is derived by mirroring the infinite geometry solution in such a way, that stresses in load direction at the straight edges are cancelled leading the flux of forces towards the clamp. To the authors' knowledge no finite dimensions problem has been treated using this mirror technique. Eventually the finite dimensions solution is verified using commercial FE software.

2 Airy stress function

In plane strain or plane stress elasticity problems equilibrium, Hooke's law and compatibility can be reduced to a single governing equation. If the material behaviour is isotropic or quasi-isotropic this equation can be expressed by a single unknown F called *Airy stress function* and the single governing equation in case of plane stress with non existent body forces reads

$$\Delta\Delta F = \frac{\partial^4 F}{\partial x^4} + 2\frac{\partial^2 F}{\partial x^2 \partial y^2} + \frac{\partial^4 F}{\partial y^4} = 0 \quad (1)$$

in cartesian coordinates,

$$\Delta\Delta F = \left(\frac{\partial^2}{\partial r^2} + \frac{1}{r}\frac{\partial}{\partial r} + \frac{1}{r^2}\frac{\partial^2}{\partial \varphi^2}\right)^2 F = 0 \quad (2)$$

in polar coordinates [6, 10, 11]. These equations (1), (2) are called *biharmonic equation*. All functions obeying the *biharmonic equation* are called *biharmonic functions* and were addressed by Michell [7] but can be also found in [11]. The plane stresses are derived using the relations

$$\sigma_x = \frac{\partial^2 F}{\partial y^2}, \quad \sigma_y = \frac{\partial^2 F}{\partial x^2}, \quad \tau_{xy} = -\frac{\partial^2 F}{\partial x \partial y}, \quad (3)$$

$$\sigma_r = \frac{1}{r}\frac{\partial F}{\partial r} + \frac{1}{r^2}\frac{\partial^2 F}{\partial \varphi^2}, \quad \sigma_\varphi = \frac{\partial^2 F}{\partial r^2}, \quad \tau_{r\varphi} = -\frac{\partial}{\partial r}\left(\frac{1}{r}\frac{\partial F}{\partial \varphi}\right). \quad (4)$$

Biharmonic functions are now to be chosen in such a way that the derived stresses fulfil the boundary conditions for a given plane elasticity problem.

3 Stress analysis for an isotropic single hole bolted joint connection

The Airy stress function for an isotropic single hole bolted joint connection under in-plane loading as shown in Fig. 1 is developed. The parameters width w, end distance e, diameter d of the circular hole and the Poisson's ratio ν are required to develop the analytical solution. The dimensions are chosen so that stress concentrations due to finite width effects faded away. Their values can be taken from Tab. 1.

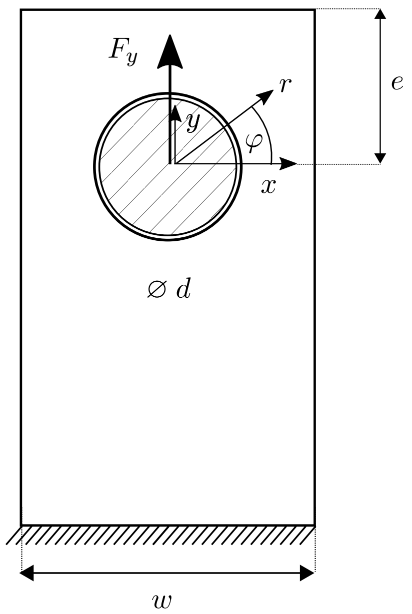

Fig. 1: Geometry of bolted joint

property	d	w/d	e/d	ν	F_y
value	2 mm	20	10	0.3	2 N

Tab. 1: Structural properties

3.1 Idealisation of the bolt plate contact problem

The bolt plate contact problem is approximated by a sinusoidal contact stress distribution over the upper half of the hole boundary as in [12]. Hence, the radial stress at the hole boundary can be written as

$$\sigma_r(R,\varphi) = -\hat{\sigma}_r \sin\varphi \quad \text{for} \quad 0 \leq \varphi \leq \pi \quad (5)$$

where $\hat{\sigma}_r$ denotes the amplitude of the stress distribution. Assuming no friction the vertical equilibrium between the load F_y and the radial contact stresses $\sigma_r(R,\varphi)$ at the bolt boundary $r = R$ requires

$$\begin{aligned} R\int_0^\pi \sigma_r(R,\varphi)\sin\varphi\,\mathrm{d}\varphi &= -F_y \\ \Leftrightarrow \quad R\int_0^\pi -\hat{\sigma}_r \sin^2\varphi\,\mathrm{d}\varphi &= -R\frac{\pi}{2}\hat{\sigma}_r = -F_y \quad (6) \\ \Leftrightarrow \quad \hat{\sigma}_r &= \frac{2}{\pi}\frac{F_y}{R}. \end{aligned}$$

The complete boundary conditions on the hole edge are expressed by

$$\begin{aligned} \sigma_r(R,\varphi) &= \begin{cases} -\frac{2}{\pi}\frac{F_y}{R}\sin(\varphi) & \text{for} \quad 0 \leq \varphi \leq \pi \\ 0 & \text{for} \quad \pi \leq \varphi \leq 2\pi, \end{cases} \\ \tau_{r\varphi}(R,\varphi) &= \quad 0 \qquad\qquad \text{for} \quad 0 \leq \varphi \leq 2\pi. \end{aligned} \quad (7)$$

At first a solution for the problem of a bolted joint with infinite dimensions is developed. This task involves finding a stress field satisfying the boundary stress conditions at the hole. To implement a finite geometry joint the solution for infinite dimensions is then mirrored in such a way that all stresses in load direction at the location of the straight edges are cancelled. Thus the flux of forces is led towards the clamp at the bottom providing a correct load transfer.

3.2 Stress field for a joint with infinite dimensions

To model the sinusoidal radial stresses at the hole boundary an approach similar to [4] is used. The solution for the Airy stress function contains two parts, $F^\infty = F_1^\infty + F_2^\infty$. At the hole boundary F_1^∞ represents a full sinusoidal radial stress distribution in compression within the contact area $(0 \leq \varphi \leq \pi)$ and in tension in the no contact area $(\pi \leq \varphi \leq 2\pi)$. F_1^∞ is calibrated so that its radial stresses at the upper hole boundary are transferring half of the outer load. F_2^∞ is a Fourier series describing a sinusoidal pressure in both areas carrying the remaining half of F_y at the upper hole boundary. Therefore both partial solutions superimposed provide transfer of the whole load F_y at the contact area whereas at the no contact area the radial stresses are cancelled. Refer to Fig. 2 for details.

The stress function F_1^∞ according to [1] is

$$F_1^\infty(r,\varphi) = a_{15}\, r\varphi\cos\varphi + b_{12}\, r\ln r\sin\varphi + b_{13}\,\frac{1}{r}\sin\varphi. \tag{8}$$

The corresponding stresses $\sigma_{r1}^\infty, \sigma_{\varphi 1}^\infty, \tau_{r\varphi 1}^\infty$ are derived using relation (4). Furthermore the coefficients a_{15}, b_{12}, b_{13} are determined by

$$\frac{b_{12}}{a_{15}} = \tfrac{1}{2}(1-\nu) \tag{9}$$

ensuring single valued circumferential displacements $u_\varphi(R,\varphi)$ [1, 10],

$$\sigma_{r1}^\infty(R,\pi/2) = -\frac{1}{\pi}\frac{F_y}{R} \tag{10}$$

transferring $F_y/2$ and eventually

$$\tau_{r\varphi 1}^\infty(R,\varphi) = 0 \tag{11}$$

ensuring vanishing shear stresses at the hole boundary. Let us express all stress functions using a reference stress value $\sigma_0 = \frac{F_y}{d}$. F_1^∞ then reads

$$F_1^\infty(r,\varphi) = \frac{R}{\pi}\Big[r\varphi\cos\varphi + \\ + \frac{1}{2}(1-\nu)\, r\ln r\sin\varphi + \frac{1}{4}(1-\nu)\, R^2\frac{1}{r}\sin\varphi\Big]\sigma_0. \tag{12}$$

The general form of F_2^∞ is

$$F_2^\infty(r,\varphi) = R^2\Big[e_0\ln\frac{r}{R} + \\ + \sum_{n=1}^{N}\Big\{D_n\left(\frac{R}{r}\right)^{2n} + E_n\left(\frac{R}{r}\right)^{2n-2}\Big\}\cos 2n\varphi\Big]\sigma_0. \tag{13}$$

The stresses determined by F_2^∞ are

$$\sigma_{r2}^\infty(r,\varphi) = \Big[e_0\left(\frac{R}{r}\right)^2 - \\ - 2\sum_{n=1}^{N}\Big\{n(2n+1)D_n\left(\frac{R}{r}\right)^{2n+2} + \\ + (n+1)(2n-1)E_n\left(\frac{R}{r}\right)^{2n}\Big\}\cos 2n\varphi\Big]\sigma_0, \tag{14}$$

$$\sigma_{\varphi 2}^\infty(r,\varphi) = \Big[-e_0\left(\frac{R}{r}\right)^2 + \\ + 2\sum_{n=1}^{N}\Big\{n(2n+1)D_n\left(\frac{R}{r}\right)^{2n+2} + \\ + (n-1)(2n-1)E_n\left(\frac{R}{r}\right)^{2n}\Big\}\cos 2n\varphi\Big]\sigma_0, \tag{15}$$

$$\tau_{r\varphi 2}^\infty(r,\varphi) = -2\Big[\sum_{n=1}^{N}\Big\{n(2n+1)D_n\left(\frac{R}{r}\right)^{2n+2} + \\ + n(2n-1)E_n\left(\frac{R}{r}\right)^{2n}\Big\}\sin 2n\varphi\Big]\sigma_0. \tag{16}$$

The coefficients D_n and E_n are calculated by representing $\sigma_{r1}^\infty(R,\varphi)$ as a Fourier series while contrary to [4] simultaneously maintaining shear stresses zero at the hole boundary. In particular

$$\sigma_{r2}^\infty(R,\varphi)/\sigma_0 = \frac{a_0}{2} + \sum_{n=1}^{N^*} a_n\cos n\varphi \tag{17}$$

with

$$a_n = \frac{2}{\pi}\frac{1}{\sigma_0}\int_0^\pi \sigma_{r1}^\infty(R,\varphi)\cos n\varphi\,\mathrm{d}\varphi \\ = -\frac{4}{\pi^2}\int_0^\pi \sin\varphi\cos n\varphi\,\mathrm{d}\varphi \quad n = 0,1,\ldots,\infty. \tag{18}$$

Equating the dimensionless radial stresses using Eq. (14) with the Fourier series representation in relation (17) and taking into account that uneven Fourier coefficients a_n are zero,

$$a_n = 0 \quad \text{for} \quad n = 1, 3, ..., \infty, \tag{19}$$

yields

$$\begin{aligned} \sigma_{r2}^{\infty}(R,\varphi)/\sigma_0 &= e_0 - 2\sum_{n=1}^{N}\Big\{n(2n+1)D_n + \\ &\quad + (n+1)(2n-1)E_n\Big\}\cos 2n\varphi \\ &= \frac{a_0}{2} + \sum_{n=1}^{N} a_{2n}\cos 2n\varphi. \end{aligned} \tag{20}$$

Equating each coefficient leads to

$$e_0 = \frac{a_0}{2}, \tag{21}$$

$$-2\{n(2n+1)D_n + (n+1)(2n-1)E_n\} = a_{2n}. \tag{22}$$

To ensure vanishing shear stresses at $r = R$ we set Eq. (16) to zero,

$$\begin{aligned} \tau_{r\varphi 2}^{\infty}(R,\varphi)/\sigma_0 &= -2\sum_{n=1}^{N}\Big\{n(2n+1)D_n + \\ &+ n(2n-1)E_n\Big\}\sin 2n\varphi = 0 \end{aligned} \tag{23}$$

$$\Leftrightarrow \qquad (2n+1)D_n + (2n-1)E_n = 0 \tag{24}$$

With Eq. (22) and (24) D_n, E_n can be calculated by

$$D_n = -\frac{2n-1}{2n+1}E_n, \tag{25}$$

$$E_n = \frac{1}{2}\frac{a_{2n}}{n(2n-1)-(n+1)(2n-1)}. \tag{26}$$

The resulting stresses at the hole boundary were calculated using MATHEMATICA and are presented in Fig. 2 and 3.

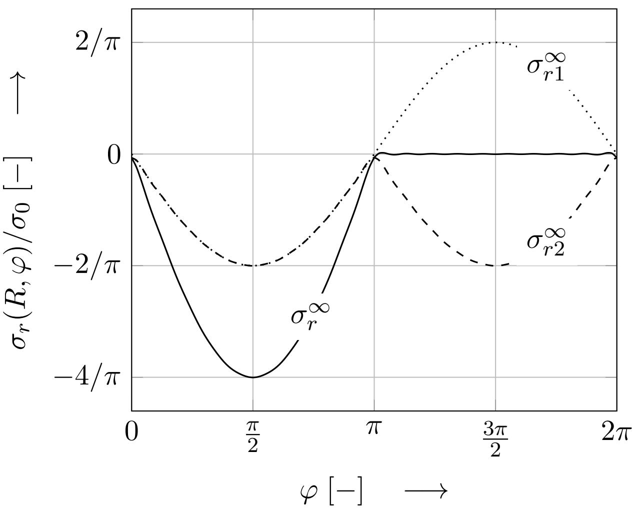

Fig. 2: Radial stresses of infinite dimensions solution using $N = 9$ Fourier coefficients

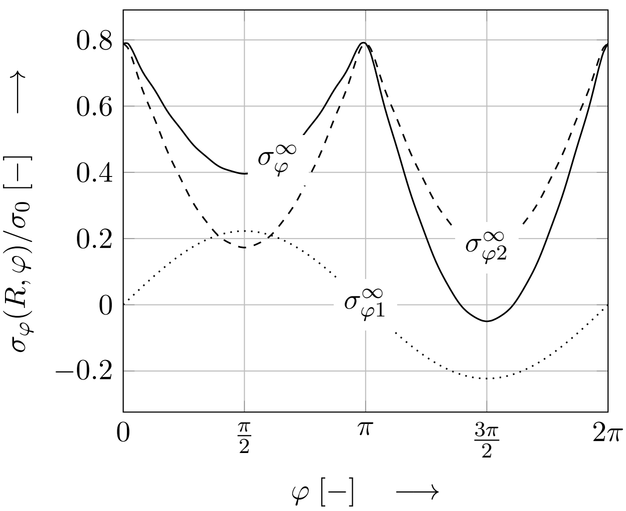

Fig. 3: Circumferential stresses of infinite dimensions solution using $N = 9$ Fourier coefficients

3.3 Stress field for a joint with finite dimensions by using a mirror technique

Let us denote the solution of infinite dimensions by F_{11}^{∞} and investigate its stresses in load direction where the straight boundaries of the joint of finite dimensions would be located. Their signs are shown in Fig. 4 obviously violating stress free boundary conditions of a finite dimensions joint. If using so called auxiliary functions or auxiliary plates by mirroring the infinite geometry solution F_{11}^{∞} as shown in this schematic those remaining stresses are cancelled.

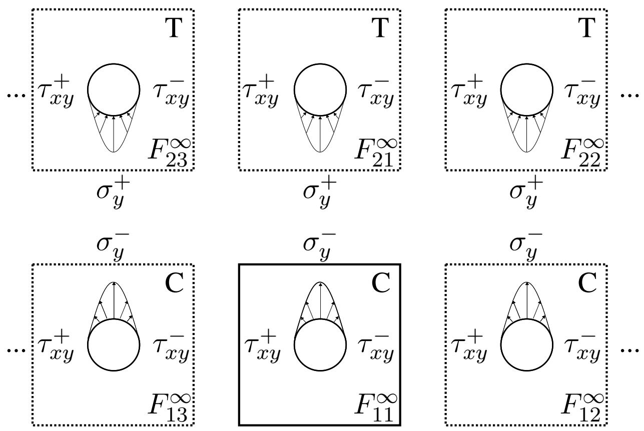

Fig. 4: Schematic how to mirror the infinite geometry solution $F^\infty = F_{11}^\infty$. C $\hat{=}$ Compression, T $\hat{=}$ Tension

To fully eliminate the remaining normal stresses σ_y^- at the horizontal edge of F_{11}^∞ the original solution needs to be vertically shifted, its sign reversed and lastly the outer sinusoidal load shifted by $180°$. This is implemented by the corresponding solution F_{21}^∞.

To cancel the remaining shear stresses at the vertical edges F_{11}^∞ has to be horizontally mirrored without changing its sign. This is incorporated by $F_{12}^\infty, F_{13}^\infty$, etc. The shear stresses of F_{11}^∞ at the right vertical edge denoted by $\tau_{xy}^{\infty 11}(w/2, y)$ are fully eliminated by just superimposing the directly opposite auxiliary plate F_{12}^∞. Elimination of the shear stresses at the left hand side edge requires an auxiliary plate solution F_{13}^∞ inducing a remaining rest in $\tau_{xy}^{\infty 11}(w/2, y)$. The same applies for cancelling shear stress at the left hand side edge. If a periodic row of horizontal auxiliary plates are used the superimposed shear stresses at the vertical boundaries will vanish. Since the shear stress cancelling auxiliary plates $F_{1,j}^\infty|_{j\neq 1}$ also induce normal stresses σ_y^- they require the upper auxiliary functions $F_{2,j}^\infty|_{j\neq 1}$ ensuring zero normal stresses.

Let us store all stress functions of the infinite geometry in a matrix $[F_{ij}^\infty]$

$$[F_{ij}^\infty] = \begin{bmatrix} F_{11}^\infty & F_{12}^\infty & F_{13}^\infty & \dots \\ F_{21}^\infty & F_{22}^\infty & F_{23}^\infty & \dots \end{bmatrix} \qquad (27)$$

where $F_{11}^\infty = F^\infty$ denotes the original Airy stress function and $F_{ij}^\infty|_{i,j\neq 1}$ the auxiliary stress functions, then F_{ij}^∞ is eventually obtained by

$$F_{ij}^\infty(x, y) = (-1)^{i+1} F^\infty\Big((-1)^{i+1} x_j, (-1)^{i+1} y_i\Big) \qquad (28)$$

with

$$[x_j] = \begin{bmatrix} x_1 \\ x_2 \\ x_3 \\ x_4 \\ \dots \end{bmatrix} = \begin{bmatrix} x \\ x - w \\ x + w \\ x - 2w \\ \dots \end{bmatrix}, \; [y_i] = \begin{bmatrix} y_1 \\ y_2 \end{bmatrix} = \begin{bmatrix} y \\ y - 2e \end{bmatrix} \qquad (29)$$

enabling the translation of F^∞. The finite dimensions solution is then built by

$$F^{\mathrm{fd}}\Big|_{n_x|n_y=2} = \sum_{j=1,2,\dots}^{n_x} (F_{1j}^\infty + F_{2j}^\infty) \qquad (30)$$

where n_x denotes the total number of horizontally, n_y the total number of vertically aligned plates.

Residual shear stresses at the vertical edges of the finite dimensions solution raise the question how many horizontally mirrored plates are required to model the load transfer accurately. To asses this matter let us investigate the stresses of the free body sketch in Fig. 6. If all stress boundary conditions are ideally fulfilled the outer load F_y must be fully transferred by the net section stresses $\sigma_y(x, 0)$. Let χ_{σ_y} be the load transfer ratio by those net section stresses,

$$\chi_{\sigma_y} = \frac{2}{F_y} \int_R^{w/2} \sigma_y^{\mathrm{fd}, n_y|n_x}(x, 0)\, \mathrm{d}x, \qquad (31)$$

where $\sigma_y^{\mathrm{fd}, n_y|n_x}$ represents the corresponding stress components of the superimposed finite geometry solution containing $n_x, n_y = 2$ plates in total. χ_{σ_y} is plotted with respect to n_x in Fig. 5 and ideally would reach 1.

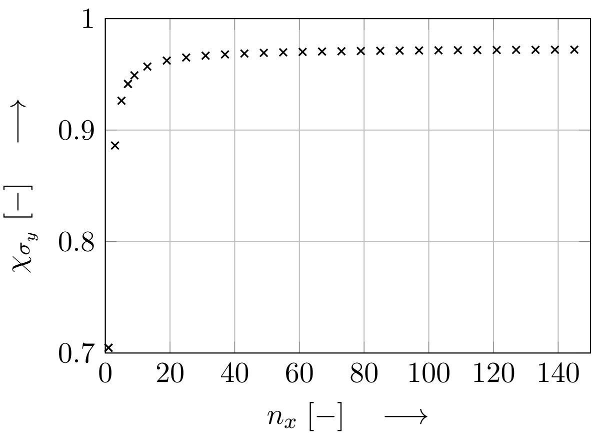

Fig. 5: Load transfer ratio for $N = 9, n_y = 2$

A load transfer value of at least 95 % is considered as sufficiently accurate which is reached for $n_x \geq 9, n_y = 2$. The lack of arriving at $\chi_{\sigma_y} = 1$ is due to the auxiliary plates apart from cancelling stresses at the straight edges to a value near zero also slightly interfering with the hole boundary stresses, which becomes evident in the superimposed radial stresses plotted in Fig. 11 as well as in the load transfer ratios of the stresses corresponding to the free form body. In particular

$$\chi_{\sigma_r} = \frac{R}{F_y}\left| \int_0^{\pi} \sigma_r^{\mathrm{fd},2|9}(R,\varphi)\sin\varphi \,\mathrm{d}\varphi \right| = 0.96 \neq 1, \tag{32}$$

$$\chi_{\tau_{r\varphi}} = \frac{R}{F_y}\left| \int_0^{\pi} \tau_{r\varphi}^{\mathrm{fd},2|9}(r,\varphi)\cos\varphi \,\mathrm{d}\varphi \right| = 0, \tag{33}$$

$$\chi_{\tau_{xy}} = \frac{1}{F_y}\left| \int_0^{e} \tau_{xy}^{\mathrm{fd},2|9}(w/2,y) - \right.$$

$$\left. - \tau_{xy}^{\mathrm{fd},2|9}(-w/2,y)\,\mathrm{d}y \right| = 0.03 \neq 0 \tag{34}$$

meaning that in the hole boundary conditions the radial stresses show the strongest deviation.

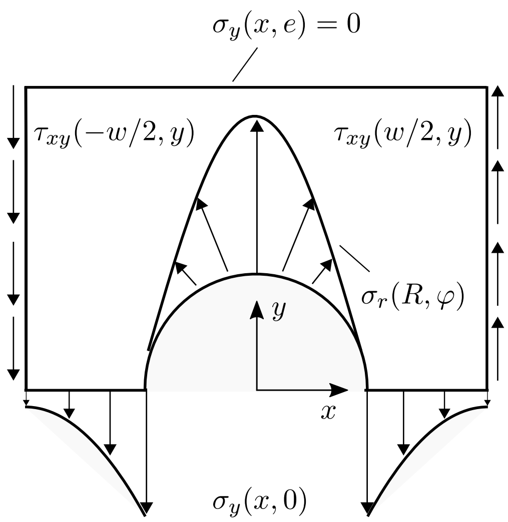

Fig. 6: Free form body - only with stresses relevant for equilibrium in load direction

To further investigate how the flux of forces is changed by mirroring the infinite geometry solution the stream plots of the stress vector

$$\vec{t_y} = \begin{bmatrix} \sigma_x & \tau_{xy} \\ \tau_{xy} & \sigma_y \end{bmatrix} \cdot \begin{bmatrix} 0 \\ -1 \end{bmatrix} = - \begin{bmatrix} \tau_{xy} \\ \sigma_y \end{bmatrix} \tag{35}$$

in Fig. 7, 8 and 9 shall serve.

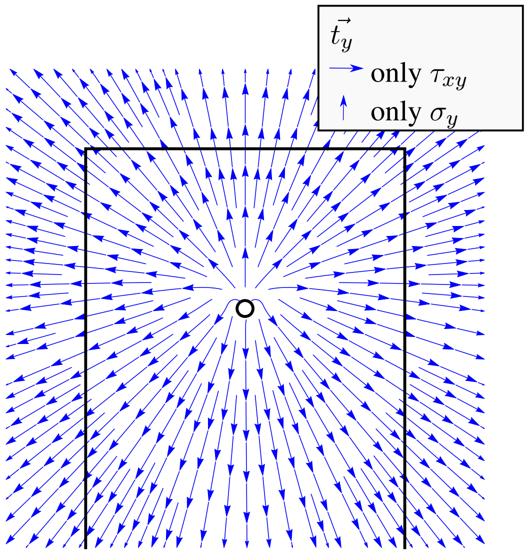

Fig. 7: Stress vectors $\vec{t_y}$ for the infinite geometry solution

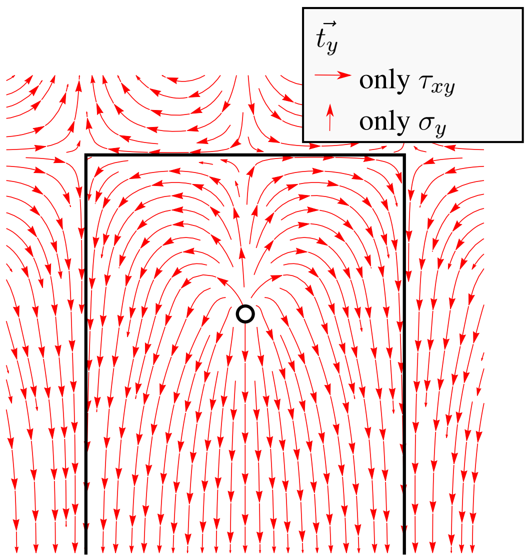

Fig. 8: Stress vectors $\vec{t_y}$ for the finite geometry solution with $n_x = 2, n_y = 21$

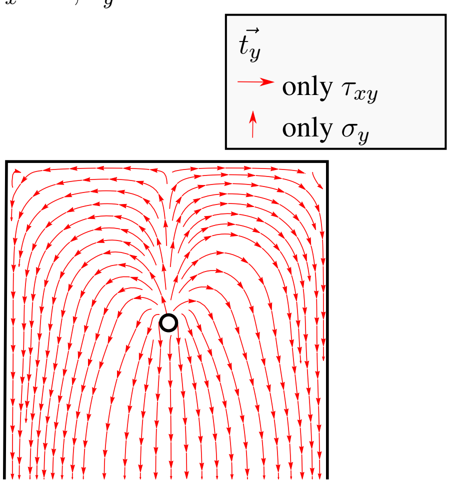

Fig. 9: Stress vectors $\vec{t_y}$ for the FE solution

Mirroring the infinite solution leads to stress vectors $\vec{t_y}$ tangent to the straight edges like those in the FE reference thus providing an accurate load transfer.

4 Comparison to Finite Element results

To verify the analytically derived stress field a two-dimensional bolted joint model is built using the FE software ABAQUS as shown in Fig. 10. The mesh contains CPS8 continuum plane stress elements with eight nodes. Furthermore a contact algorithm in between plate and bolt as well as a sinusoidal contact stress distribution are implemented providing justification of this contact problem idealisation. Convergence of the stresses at the hole boundary is assumed if an increase of the number of the elements leads to unnoticeable changes in those stresses. This is reached for at least 72 elements at the hole boundary. The plate is modelled as a quasi-isotropic composite laminate of T300/Epoxy with effective stiffness parameters E, ν. The bolt material is titanium characterised by $E_{\mathrm{B}}, \nu_{\mathrm{B}}$. Tab. 2 shows the implemented effective stiffness values.

property	E [MPa]	ν [-]	E_{B} [MPa]	ν_{B} [-]
value	57 890	0.3	110 000	0.3

Tab. 2: Stiffness properties

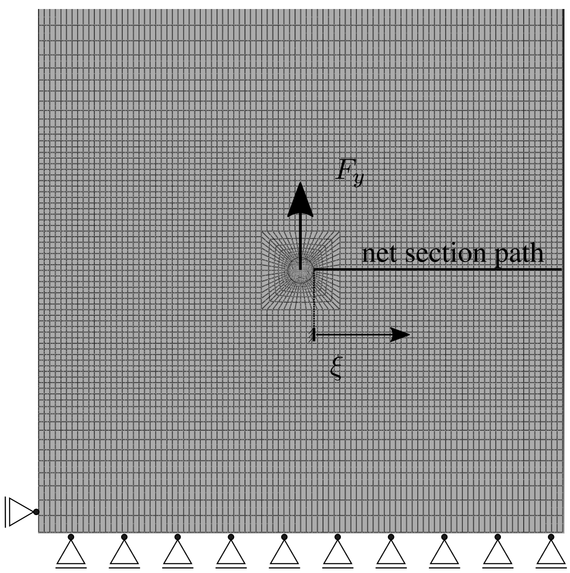

Fig. 10: Finite element model

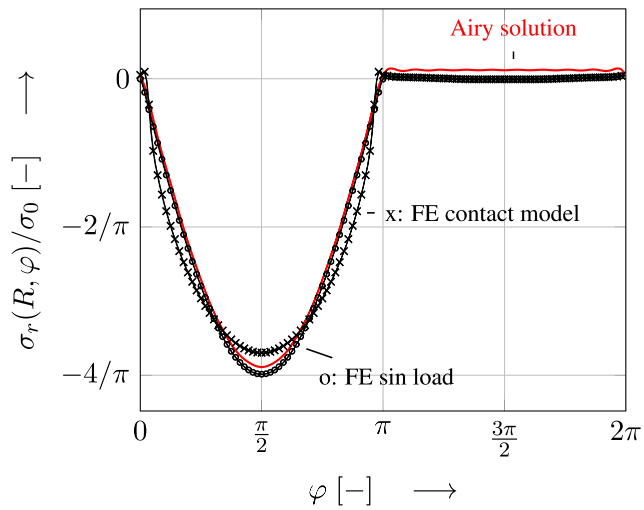

Fig. 11: Comparison to FE results: radial stresses

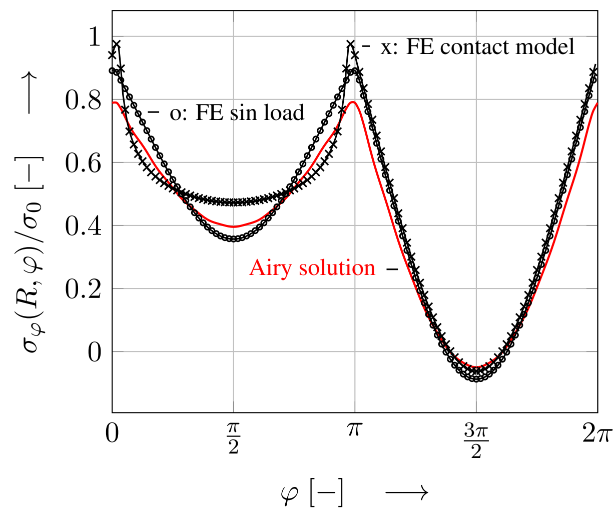

Fig. 12: Comparison to FE results: Circumferential stresses

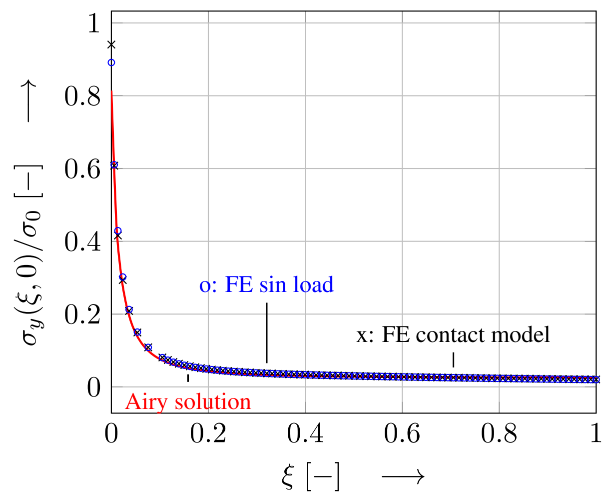

Fig. 13: Comparison to FE results: stresses in load direction at net section

The net section stresses are plotted with respect to the dimensionless coordinate

$$\xi = \frac{x - R}{w/2 - R} \qquad (36)$$

shown in Fig. 10 with $\xi = 0$ at the hole boundary and $\xi = 1$ at the right vertical edge.

The radial stresses and tangential stresses in Fig. 11 and 12 at the hole boundary as well as the net section stress in Fig. 13 show that the bolt plate contact idealisation as sinusoidal stress distribution and therefore the reduction of the nonlinear contact problem to a linear problem is acceptable for the given isotropic configuration with quasi infinite dimensions.

The present solution provides a good approximation of the tangential stresses although not hitting the peaks at the net section area $\varphi = \{0, \pi\}$. Since in net section failure assessment by common means like Theory of Critical Distances [9] or Finite Fracture Mechanics [13] stresses at or within a certain distance d_0 but not only directly at the hole boundary play a role this drawback can be considered as tolerable. Moreover the very good agreement of the net section stresses in Fig. 13 shows that the present solution provides an adequate means for 2D stress analysis and subsequent net tension failure assessment.

5 Conclusion

A closed-form analytical solution for a pin-loaded hole in an isotropic plate with finite dimensions has been developed by means of the Airy stress function. The geometry is chosen in such a way that additional stress concentrations due to finite dimensions faded away. The pin-plate contact problem is idealised by a sinusoidal distribution in the radial stresses. Firstly a solution for the infinite geometry fulfilling the hole boundary conditions is derived. Afterwards the finite geometry problem is treated by mirroring the infinite dimensions solution in such a way that stresses in load direction at the straight edges of the plate are cancelled. Unfortunately superimposed mirrored stress fields also slightly change the hole boundary conditions. Nevertheless the comparison to FE results shows that the present finite geometry solution still accurately models the load transfer towards the clamp as well as characteristic field quantities and therefore provides an efficient tool for 2D stress analysis.

References:

[1] W. G. Bickley, *The Distribution of Stress Round a Circular Hole in a Plate,* Philosophical Transactions of the Royal Society of London. Series A, Vol. 227, 383-415.

[2] T. de Jong *Stresses around pin-loaded holes in elastically orthotropic or isotropic plates,* J. Compos. Mater., 1977, 11, 313-331.

[3] B. Grüber, W. Hufenbach et. al., *Stress concentration analysis of fibre-reinforced multilayered composites with pin-loaded holes,* Composites Science and Technology 67 (2007), 1439-1450.

[4] R. C. Knight, *The action of a rivet in a plate of finite breadth,* Philosophy Magazine, 19 (Series 7) (1935), 517-540.

[5] S. Lekhnitskii, *Anisotropic plates,* New York: Gordon and Breach Science Publishers; 1968.

[6] W. Becker and D. Gross, *Mechanik elastischer Körper und Strukturen,* Springer, Berlin, 2002.

[7] J. H. Michell, *On the direct determination of stress in an elastic solid with application to the theory of plates,* Proc. London Math. Soc., vol 31 1899, 100-124.

[8] J. Ogonowski, *Effect of variances and manufacturing tolerances on the design strength and life of mechanically fastened composite joints,* Tech. Rep. AFWAL-TR-81-3041, vol. 3, McDonnell Aircraft Company; 1981.

[9] D. Taylor, *The Theory of Critical Distances,* Elsevier Science, Oxford, London 2007.

[10] S. Timoshenko and J. N. Goodier, *Theory of Elasticity,* McGraw-Hill Book Company, Inc., New York, 1951.

[11] M. H. Sadd, *Elasticity: Theory, Applications, and Numerics* Elsevier Butterworth-Heinemann, Burlington, 2005.

[12] J. P. Waszczak and T. A. Cruse, *Failure mode and strength prediction of anisotropic bolt bearing specimens,* J Compos Mater 1971; 5: 421-425.

[13] P. Weißgraeber, D. Leguillon and W. Becker, *A review of Finite Fracture Mechanics: crack initiation at singular and non-singular stress raisers,* Arch Appl Mech (2016) 86:375-401.